Research Article | Vol. 30, No. 10 / 9 May 2022 / Optics Express 16499
Optics EXPRESS

Dual-band fiber optic parametric amplifier for bi-directional transient-sensitive fiber optical transmission links

CHANDRA B. GAUR,[1,2] VLADIMIR GORDIENKO,[1,*] AND NICK J. DORAN[1]

[1]Aston Institute of Photonics Technology, Aston University, Birmingham, B4 7ET, UK
[2]Now with SubCom LLC, 250 Industrial Way W, Eatontown, NJ 07724, USA
[*]v.gordienko1@aston.ac.uk

Abstract: We demonstrate an in-line polarization-insensitive fiber optic parametric amplifier (PI-FOPA) to simultaneously amplify burst and non-burst signals transmitted in opposite directions in C and L bands. The PI-FOPA provides >16 dB polarization insensitive net gain for signals which are 53 nm apart and counter-propagating in an extended reach link: an upstream bursty signal at 1533 nm and a downstream non-burst signal at 1586 nm. The PI-FOPA potential application as an in-line dual-band amplifier in transient-sensitive communication links is demonstrated by its employment in an extended reach access network with a symmetric 10 Gbps capacity.

1. Introduction

Modern optical communications require amplifiers for multi-band operation to satisfy an ever-growing demand for capacity [1]. Besides, many of fiber optic communication links are transient-sensitive, i.e., time-varying signals in such links can be degraded by transients in optical amplifiers. For example, future reach extended access networks are envisaged to require amplification of bursty signal channels coarsely multiplexed across several bands [2] hence they will require an amplifier with multi-band capability and with fast response time to prevent transients corrupting data [3]. However, such an amplifier is a serious challenge because current doped fiber, Raman and semiconductor amplifiers have limitations attributed to operation bandwidth and/or transient effects [4–7].

We consider a fiber optic parametric amplifier (FOPA) to be a strong candidate for multi-band transient-sensitive fiber optic communications for several reasons. FOPAs can operate in any telecom band [8] with ultra-wide gain bandwidth in excess of 200 nm using a single pump source [9,10]. FOPAs cause little penalty when amplifying time-varying data signals due to its ultra-fast response time of ~0.1 fs and gain independent of signal power [11]. Additionally, FOPAs can provide phase-sensitive amplification with ~0 dB noise figure [12,13], large signal gains up to 70 dB [14] and large output power [15].

Recent advancement of looped polarization insensitive FOPAs [16] has enabled them to significantly outperform EDFAs and fiber Raman amplifiers in terms of signal quality when amplifying bursty traffic with gain up to 20 dB [17]. Although EDFA has allowed for ~1 dB better received sensitivity than PI-FOPA when amplifying continuous traffic [4], the PI-FOPA has improved receiver sensitivity by up to 5 dB [4] or five-folded the link capacity [18] when employed as a drop-in replacement for EDFA in a reach extended access network transmitting signal bursts.

However, these PI-FOPA demonstrations of transient-free operation have been performed with a single unidirectional channel, whilst many of fiber optic links operate over wide bandwidth and

#458166 https://doi.org/10.1364/OE.458166
Journal © 2022 Received 10 Mar 2022; revised 14 Apr 2022; accepted 19 Apr 2022; published 28 Apr 2022

Optics EXPRESS

transmit data in both directions [19]. FOPAs in most demonstrations exhibit only unidirectional gain due to the phase-matching requirement [20]. Although bi-directional gain can, in principle, be obtained by launching pumps in both directions [21], high power pumps counter-propagating at close frequencies can interact via a combination of backscattering and four-wave mixing [22]. This leads to an aggravation of stimulated Brillouin scattering, generation of significant pump noise and eventually has a devastating impact on signal amplification when the parametric gain is high [22].

In this work, we demonstrate an in-line PI-FOPA to simultaneously amplify signals in C and L bands, both burst and non-burst, using our original configuration for bi-directional dual-band PI-FOPA operation. We employ this PI-FOPA in a 50 km reach access link with symmetric 10 Gbps capacity to provide >16 dB polarization-insensitive net gain for an upstream bursty 10G on-off keying (OOK) signal at 1533 nm and a downstream non-burst 10G OOK signal at 1586 nm. The PI-FOPA in a bi-directional arrangement consequently improves the link power budget by 14 dB. This work presents an important step towards PI-FOPA implementation in broadband links with bi-directionally transmitted signals. This paper extends our conference publication [23] and focuses on dual-band bi-directional operation. We have also explored this configuration in our recent conference paper [24] for WDM applications.

2. Experimental setup

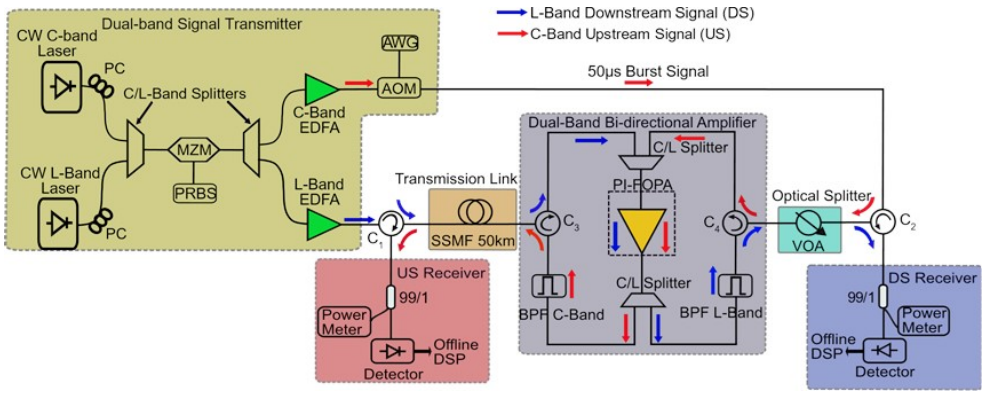

Fig. 1. Experimental setup of reach extended access link employing dual-band bi- directional polarization-insensitive FOPA as an in-line amplifier

Figure 1 shows the experimental setup of a reach extended access link employing a dual-band PI-FOPA for dual band signal amplification and bi-directional transmission. The setup consisted of a C and L band transmitter, a 50 km transmission span, a dual-band PI-FOPA in a bi-directional arrangement, an optical splitter, and optical signal detectors to receive individual L-band and C-band counter-propagating signals respectively. The dual-band transmitter generates a continuous 10 Gbps OOK signal in the L band for downstream (DS) and a bursty 10 Gbps OOK signal in the C band for upstream (US). The signal carrier waves are sourced from two 100 kHz linewidth tunable lasers tuned to 1586 nm and 1533 nm respectively and multiplexed via a C/L-band splitter. Then, the carrier waves are amplitude-modulated with a single Mach-Zehnder modulator (MZM) driven by a pseudo-random bit sequence (PRBS) to produce 10G OOK signals. The carrier waves polarizations were controlled independently to minimize their insertion loss in the MZM. The modulated signals were de-multiplexed with another C/L band splitter and amplified by corresponding C and L band EDFAs. The US channel was then passed through an acousto-optic modulator (AOM) driven by a 10 kHz square wave with a duty cycle (DC) of 50% to generate 50

Optics EXPRESS

μs long bursts with a period of 100 μs. The average US signal power was 2.5 dBm at 50% DC, which corresponds to the burst signal power of 5.5 dBm. The DS signal power was 6 dBm. There was no need to deliberately de-correlate the signals produced by the same modulator because they are counter-propagating in the link.

The DS channel was launched into the 50 km standard single-mode fiber (SSMF) transmission span via an optical circulator C_1, amplified by the bi-directional PI-FOPA arrangement, passed through an optical splitter emulated by a variable optical attenuator (VOA), and propagated to the DS receiver via an optical circulator C_2. The US channel has followed the same path in the reversed order: it was injected in the optical splitter via the optical circulator C_2, amplified by the bi-directional FOPA arrangement, transmitted over the 50 km SSMF span, and then guided to the US receiver via the optical circulator C_1. The 50 km span had insertion loss of ~9.7 dB at the channel wavelength of 1533 nm and ~9.8 dB at 1586 nm.

The received DS and US signals are detected by a DC-coupled direct detection PIN photodiode with a responsivity of 0.7 AW^{-1} and bandwidth of 30 GHz. The detector was connected to a 23 GHz real-time oscilloscope for capturing signal traces. Offline digital signal processing (DSP) was employed to detect bursts, define decision threshold, discard bits corrupted by AOM when producing signal bursts, and to find the bit error ratio (BER) [4].

Inherently our PI-FOPA is a uni-directional amplifier, so it was employed in our original arrangement employing a set of circulators and band splitters to amplify signals counter-propagating in the transmission link (Fig. 1). Optical circulators C_3 and C_4 were employed to separate counter-propagating signals at the input and the output of the arrangement as shown in Fig. 1. Then, the signals were multiplexed using a C/L band splitter at the FOPA input, amplified by the PI-FOPA, and demultiplexed using another C/L band splitter. Finally, each amplified signal was passed through a ~1 nm wide bandpass filter (BPF) tuned to the signal wavelength to remove idlers and broadband noise generated in the FOPA. The DS and US channels had the following powers at the input and the output of the bi-directional FOPA arrangement when the VOA emulating an optical splitter was set to a minimum attenuation of 0.56 dB: the DS channel powers were -7.5 dBm and 9.9 dBm, and the US channel powers were - 2.0 dBm and 14.2 dBm respectively.

The dual-band PI-FOPA had a looped "Loss-Gain" configuration to minimize nonlinear impairments at high output signal powers (Fig. 2) [16]. An input signal launched via optical circulator was split by a polarization beam splitter (PBS) into two orthogonal polarization states. Each signal polarization state was independently and equally amplified by one of the two highly nonlinear fibers (HNLF) with lengths of 250 m and 200 m. Dispersion stable HNLFs have a zero-dispersion wavelength (ZDW) at ~1564 nm with a nonlinear coefficient of 8.2 $W^{-1}Km^{-1}$. The pumps were sourced from a tunable laser at 1564.4 nm, phase modulated with three radio frequency (RF) tones at 100, 320, and 980 MHz to mitigate SBS, and split with a 3 dB coupler. Each pump was then amplified by a high-power EDFA and coupled into corresponding HNLF via WDM couplers. Pump powers in the 250 m and 200 m HNLF lengths were 33.4 dBm and 32.7 dBm respectively. Pumps have been removed from the loop by WDM filters after propagation through HNLF. More details on the looped PI-FOPA operation are provided in [16].

Optics EXPRESS

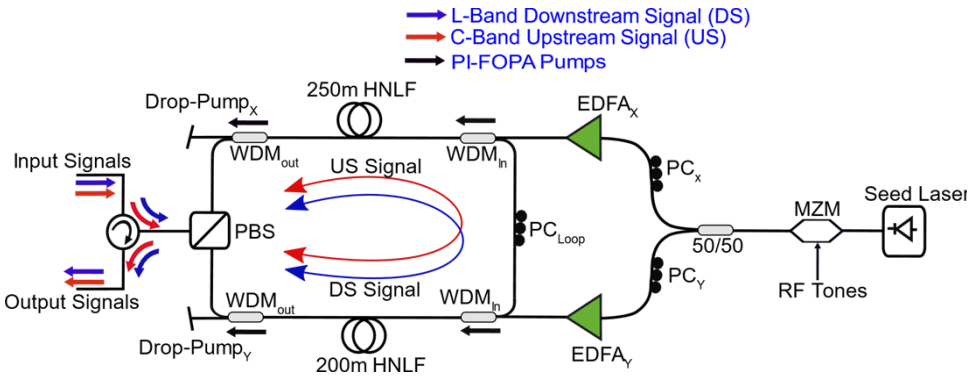

Fig. 2. Experimental setup of "Loss-Gain" polarization-insensitive FOPA

3. Results and discussion

3.1. Power spectra of amplified C and L dual-band signals

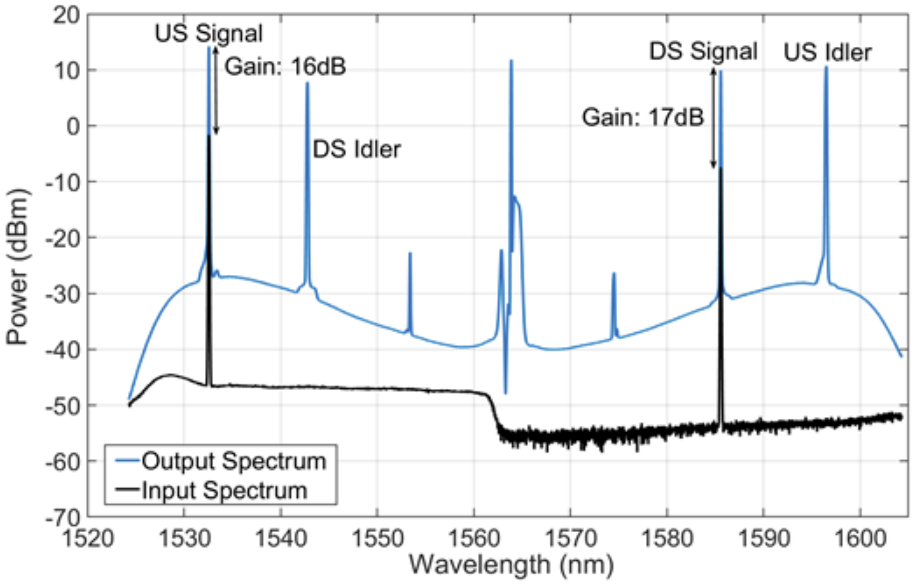

Fig. 3. Optical power spectra of dual-band signals at the input and output of PI-FOPA, which demonstrate 16 dB net gain for C-band US signal and 17 dB net gain for L-band signal.

Figure 3 shows power spectra at the input and output of the PI-FOPA measured with optical spectrum analyzer resolution bandwidth of 0.1 nm. The optical splitter attenuation was set to the minimum of 0.56 dB, which leads the maximum powers of DS and US signals. Figure 3 shows amplified signals, their idlers, the residual pump, and unwanted products of FWM between the signals. It can be derived that the PI-FOPA provides net gain across ~80 nm (~10 THz) bandwidth between 1525 nm to 1605 nm. However, it is required to have close high gain values for the DS and US channels, no polarization-dependent gain for both channels and a sufficient guard band of at least ~10 nm between the signals and idlers to simplify their filtering. We have found it possible to satisfy all these requirements at signal wavelengths of 1533 nm and 1586 nm and to obtain polarization-insensitive gains of 15.9 dB and 17.4 dB respectively. Polarisation

Optics EXPRESS

dependent gain (PDG) for both DS and US channels were around 0 dB. PDG was calculated by subtracting X and Y arm gain of a looped PI-FOPA configuration as detailed in [16]. The idler wavelengths were 1543 nm and 1596 nm, and the residual pump was at 1564.4 nm, so they could be removed by tuneable band-pass filters with a high extinction ratio. The average output powers of the DS and US channels were 9.9 dBm and 14.2 dBm respectively. However, given the 50% duty cycle of the bursty US channel, its power during the burst was 17.2 dBm, so overall PI-FOPA output signal power during the bursts was 17.9 dBm. The US channel had higher power at the PI-FOPA input than the DS channel because the former has little loss between transmitter and the PI-FOPA, while the latter has a 50 km span between the transmitter and the PI-FOPA (Fig. 1).

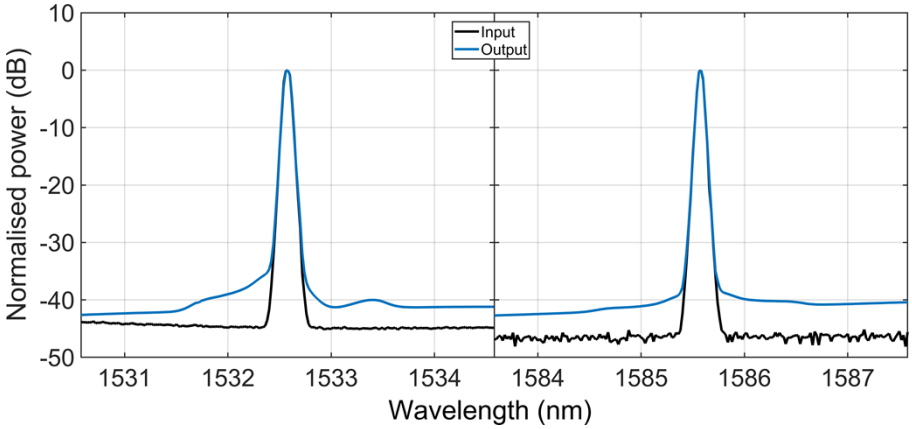

Fig. 4. Normalized optical power spectra of the signals at the input and output of the PI-FOPA show negligible signal broadening.

Figure 4 shows a close view on normalized optical power spectra of upstream C-band and downstream L-band signals before and after PI-FOPA amplification. No signal broadening was observed above the level of -35 dB. Distortions below this level are presumably attributed to the pump-to-signal noise transfer.

3.2. *Received signal spectrum of DS and US dual-band signals*

Figure 5 shows optical power spectra at the downstream and upstream detectors measured via uncalibrated 1% taps when the splitter attenuation was set to the minimum attenuation of ~0.56 dB (after ~3 dB insertion loss from BPF and C/L band WDM splitter). The plot in Fig. 5 shows received power spectra for DS and US signals and additionally shows that inter-channel crosstalk due to the limited extinction ratio of circulators and bandpass filters is low.

The DS signal reached the US receiver due to the leakage through circulator C1, whereas other unwanted waves in Fig. 5(a) leaked through the C-band BPF. Nevertheless, a high extinction ratio >30 dB was obtained between the US channel and all other waves present at the FOPA output (Fig. 5 (a)). Similarly, the US signal leaked to the DS detector through the circulator C2, and other unwanted waves leaked through the L-band BPF (Fig. 5(b)). A sufficient extinction ratio of ~20 dB was obtained between the DS signal and the US idler owing to the prescribed detuning of ~10 nm between them (b)).

3.3. *BER vs received signal power*

In this section, we discuss the performance of DS and US signals by measuring their bit error ratio (BER) against their power at the receiver. Firstly, the BER was measured for DS L-band and US C-band signals when they were transmitted one at a time. Secondly, the BER

Optics EXPRESS

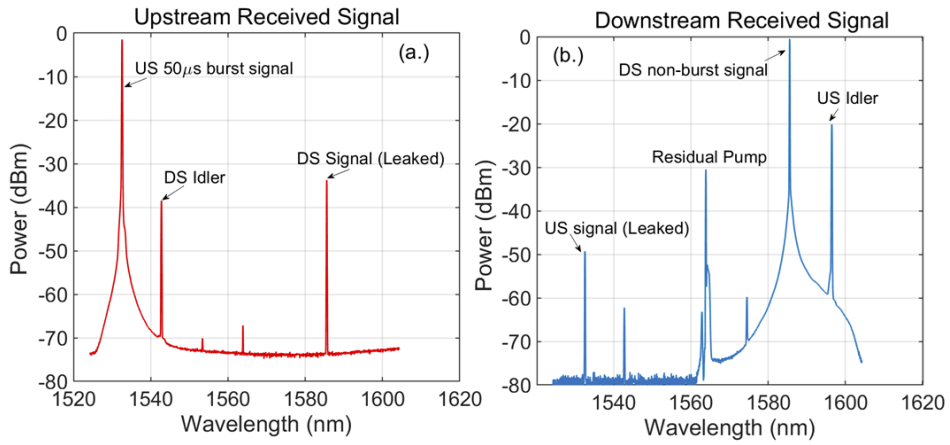

Fig. 5. Optical power spectra at a) the upstream signal photodetector and b) the downstream signal photodetector.

performance was measured for DS L-band and US C-band signals whereas they were transmitted concurrently in opposite directions. The measured BER is discussed for two different scenarios for above-mentioned cases: 1) back-to-back (B2B) excluding the 50 km span and the PI-FOPA and 2) extended reach link including the 50 km link and the PI- FOPA.

Figure 6 demonstrates performance measurement for DS and US signals transmitted one at a time. Figure 6(a) shows BER against received signal power for the L-band downstream signal transmitted at 1586 nm. First, the BER was measured in B2B for a non-burst signal transmission to set a reference point. Then, the non-burst DS signal was propagated within a complete link including in-line PI-FOPA and 50 km SMF link. The required received power difference, i.e., penalty, between the B2B and the extended reach link cases for non- burst DS signals was ~1 dB at a BER level of 10^{-3}. This penalty was induced by the 50 km SSMF attenuation and dispersion as well as the PI-FOPA noise, and it shows that the impact of these impairments on the non-burst signal was small.

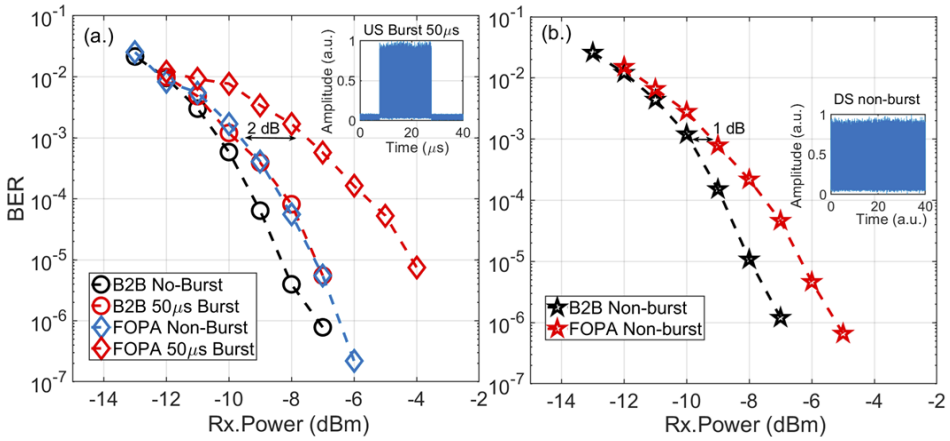

Fig. 6. BER vs received signal power for individually transmitted signals: (a) C-Band upstream signal and (b) L- band downstream signal

Optics EXPRESS

Figure 6(b) shows BER against received power measurement for US C-band signal, transmitted at 1533 nm. The US signal was transmitted uni-directionally in the setup. First, BER was measured in B2B with non-burst and 50 µs burst mode signals. The received power difference of ~1 dB was observed between non-burst and burst signals at a BER level of 10^{-3} in the B2B case. The bursty signal required a higher received signal power than the non-burst signal due to signal bursts distortions incurred by the receiver and the AOM producing bursts in the transmitter.

Then, a non-burst and a burst US signals were transmitted over the extended reach link including the 50 km span and the PI-FOPA. A received power penalty of ~1 dB was observed for the non-burst signal at the BER level of 10^{-3} as compared to the non-burst B2B case. The same penalty was observed for the non-burst DS signal (Fig. 6(a)). However, a bursty US signal demonstrated a received power penalty of ~2 dB as compared to the bursty B2B case. The penalty increase in the bursty case is attributed to the transmission and amplification of the bursty signal.

The inset of Fig. 6 (a) and (b) shows detected DS and US signals in non-burst and burst mode respectively. The traces of the signal were captured at the received signal power of -5 dBm. A waveform of the amplified 50 µs burst mode signal shows no transients due to the ultra-fast response time of the PI-FOPA [4].

In Fig. 7 we compared BER performance against received signal power for DS and US signals when both signals are transmitted simultaneously in the extended reach link. No additional penalty was observed for bi-directional transmission of these channels as compared to the results of their transmission shown in Fig. 7. Non-burst DS and US signals in the L and the C bands respectively show similar performance which agrees with previous results too. When the US C-band signal was switched to the burst mode, it has incurred a ~2 dB received power penalty at BER level of 10^{-3}. This agrees well with the case shown in Fig. 6(b) when the US signal was transmitted and amplified individually. As discussed above the additional penalty in the burst signal case is incurred by all: the transmitter, the receiver, and the in-line PI-FOPA.

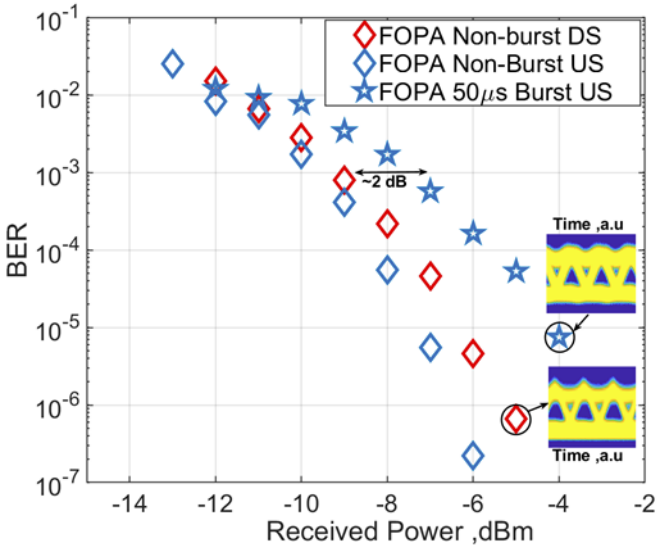

Fig. 7. BER vs received signal power for the L-band downstream and the C-band upstream signals transmitted simultaneously in opposite directions.

It is important to note that no additional penalty was incurred due to transmission and amplification of the counter-propagating signals in the C and L bands. The bi-directional PI-FOPA arrangement is, therefore, fit for amplification of signals counter-propagating in different bands with little penalty. Inset of Fig. 7 shows eye patterns of L-band DS and C-band US signals

Optics EXPRESS

measured at the power of -5 dBm. The open eye diagrams confirm viability of our original arrangement to facilitate a bi-directional dual-band operation using a uni-directional PI-FOPA.

3.4. Link power enhancement by in-line dual-band FOPA

In this section we present and discuss link power budget improvement provided by dual-band FOPA employed in a potential reach extended access link. Figure 8 characterizes the extended reach link performance by showing BER as a function of splitter loss (VOA attenuation). BER was measured for both DS and US signals as VOA attenuation was varied in the range from 10 dB to 19 dB. The maximum achievable splitter loss was measured at signal BER level of 10^{-3} for each signal. The splitter attenuation of ~16 dB was reached for both DS and US non-burst channels at the BER level of 10^{-3}. This confirms the PI-FOPA ability to simultaneously amplify signals at wavelengths >50 nm (6.5 THz) apart with the same performance. In the case of bursty US 50 µs signal, the splitter attenuation achievable at BER level of 10^{-3} decreased to 14 dB due to the 2 dB burst implementation penalty discussed above. Overall, the results obtained in Fig. 8 demonstrate the ability of the bi-directional PI-FOPA arrangement to amplify dual-band counter-propagating signals in non-burst and burst mode simultaneously. The PI-FOPA employment consequently allows for the splitter power budget of 16 dB and 14 dB for DS and US signals respectively.

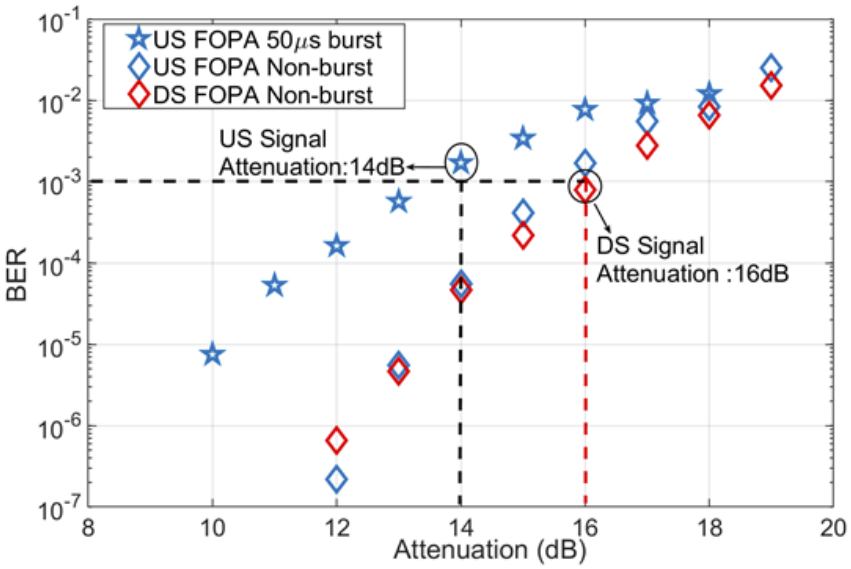

Fig. 8. BER vs splitter attenuation for the DS and US (both burst and non-burst) channels counter-propagating in the extended-reach access link. Attenuation achievable at BER of 10^{-3} denotes the available splitter budget for each case.

Figure 9 shows BER versus splitter attenuation for the 50 km reach access link with and without the PI-FOPA for (a) the non-burst DS channel and (b) the bursty US channel. Therefore, Fig. 9 allows evaluating the power budget improvement provided by the PI- FOPA addition. the splitter attenuation at BER of 10^{-3} was only ~2 dB and ~1 dB for the non-burst DS and the bursty US signals respectively after 50 km transmission without PI- FOPA. Therefore, it was not possible to place any splitter after the transmission link with the power budget available without amplification. The addition of a bi-directional dual-band PI-FOPA arrangement has enabled a splitter power budget of 14 dB for the 50 km reach access link with symmetric 10G capacity. The PI-FOPA has consequently delivered a 14 dB and 13 dB power budget improvement for the non-burst DS and the bursty US signals respectively.

Optics EXPRESS

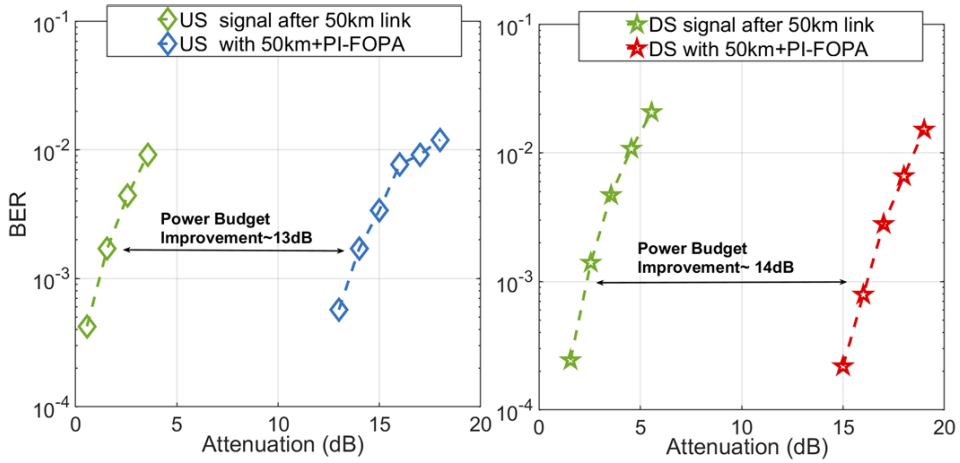

Fig. 9. BER versus splitter attenuation after transmission over the 50 km access link with and without a bidirectional dual-band PI-FOPA arrangement for (a) non-burst DS channel and (b) bursty US channel. The plot shows a link to power budget improvement provided by the PI-FOPA employment.

The demonstrated access link performance has been limited by transmitter and receiver performance especially for bursty traffic. However, the main outcome of this work is that PI-FOPA can improve performance of bi-directional broadband transient-sensitive fiber optic links.

4. Conclusion

We experimentally demonstrate a dual-band polarization-insensitive FOPA operating as in-line amplifier in a bi-directional 50 km optical fiber transmission link. An arrangement of circulators and band splitters is employed to enable bi-directional amplification using a uni-directional FOPA. The PI-FOPA delivers a polarization-insensitive net gain of 16 dB and 17 dB respectively for two >6.5 THz spaced channels at 1533 nm and 1586 nm counter-propagating in the link. Additionally, we report simultaneous FOPA amplification of a non-burst and 50 µs bursty signal in C and L telecom bands. The FOPA added as an in-line amplifier increases a splitter power budget by 14 dB for downstream non-burst signal and by 13 dB for upstream burst-mode signal. Overall, this experimental work demonstrates the suitability of PI- FOPA for in-line employment in dual-band transient-sensitive fiber optic communication links.

Funding. Engineering and Physical Sciences Research Council (FPA-ROCS (EP/R024057/1), UPON (EP/M005283/1)).

Acknowledgments. We would like to thank to Dr. Ian Philips for providing L-Band booster EDFA and Dr. Florent Bessin and Dr. Vitor Ribeiro for general lab discussions.

Disclosures. The authors declare no conflicts of interests.

Data Availability. To access the underlying data please see: [25]

References

1. N. Sambo, A. Ferrari, A. Napoli, N. Costa, J. Pedro, B. Sommerkorn-Krombholz, P. Castoldi, and V. Curri, "Provisioning in Multi-Band Optical Networks," J. Lightwave Technol. **38**(9), 2598–2605 (2020).
2. A. Shahpari, R. M. Ferreira, R. S. Luis, Z. Vujicic, F. P. Guiomar, J. D. Reis, and A. L. Teixeira, "Coherent Access: A Review," J. Lightwave Technol. **35**(4), 1050–1058 (2017).
3. K. Suzuki, Y. Fukada, T. Nakanishi, N. Yoshimoto, and M. Tsubokawa, "Burst-mode Optical Amplifier for Long-reach 10 Gbit/s PON application," in Optical Fiber Communication Conference (OFC), OSA Technical Digest (CD) (Optica Publishing Group, 2008), paper OThL3.

Optics EXPRESS

4. C. B. Gaur, F. Ferreira, V. Gordienko, V. Ribeiro, Á. D. Szabó, and N. J. Doran, "Experimental comparison of fiber optic parametric, Raman and erbium amplifiers for burst traffic for extended reach PONs," Opt. Express **28**(13), 19362–19373 (2020).
5. T. Horvath, J. Radil, P. Munster, and N. H. Bao, "Optical Amplifiers for Access and Passive Optical Networks: A Tutorial," Appl. Sci. **10**(17), 5912 (2020).
6. C. Chen and W. S. Wong, "Transient Effects in Raman Optical Amplifiers," in *Optical Amplifiers and Their Applications, OSA Technical Digest Series* (Optica Publishing Group, 2001), paper OMC2.
7. M. Shiraiwa, Y. Awaji, H. Furukawa, S. Shinada, B. J. Puttnam, and N. Wada, "Performance evaluation of a burst-mode EDFA in an optical packet and circuit integrated network," Opt. Express **21**(26), 32589–32598 (2013).
8. M. E. Marhic, K. Y. Wong, and L. G. Kazovsky, "Wide-band tuning of the gain spectra of one-pump fibre optical parametric amplifiers," IEEE J. Sel. Top. Quantum Electron. **10**(5), 1133–1141 (2004).
9. M. C. Ho, K. Uesaka, M. Marhic, and Y. Akasaka, "200-nm-bandwidth fibre optical amplifier combining parametric and Raman gain," J. Lightwave Technol. **19**(7), 977–981 (2001).
10. V. Gordienko, M. F. C. Stephens, A. E. El-Taher, and N. J. Doran, "Ultra-flat wideband single-pump Raman-enhanced parametric amplification," Opt. Express **25**(5), 4810–4818 (2017).
11. G. W. Lu, M. E. Marhic, and T. Miyazaki, "Burst-mode amplification of dynamic optical packets using fibre optical parametric amplifier in optical packet networks," Electron. Lett. **46**(11), 778–780 (2010).
12. Z. Tong, C. Lundström, P. Andrekson, C. J. McKinstrie, M. Karlsson, D. J. Blessing, E. Tipsuwannakul, B. J. Puttnam, H. Toda, and L. Gruner-Nielsen, "Towards ultrasensitive optical links enabled by low-noise phase-sensitive amplifiers," Nat. Photonics **5**(7), 430–436 (2011).
13. V. Gordienko, F. Ferreira, J. R. Lamb, Á. Szabó, and N. Doran, "Phase-sensitive amplification of 11 WDM channels across bandwidth of 8 nm in a fibre optic parametric amplifier," in 2020 European Conference on Optical Communications (ECOC).
14. T. Torounidis, P. A. Andrekson, and B. E. Olsson, "Fibre-optical parametric amplifier with 70-dB gain," IEEE Photonics Technol. Lett. **18**(10), 1194–1196 (2006).
15. S. Oda, H. Sunnerud, and P. A. Andrekson, "High efficiency and high output power fibre-optic parametric amplifier," Opt. Lett. **32**(13), 1776–1778 (2007).
16. V. Gordienko, F. M. Ferreira, C. B. Gaur, and N. J. Doran, "Looped Polarization-Insensitive Fibre Optical Parametric Amplifiers for Broadband High Gain Applications," J. Lightwave Technol. **39**(19), 6045–6053 (2021).
17. C. B. Gaur, F. Ferreira, V. Gordienko, V. Ribeiro, and N. J. Doran, "Demonstration of improved performance provided by FOPA for extended PON in burst-mode operation," in 2019 European Conference on Optical Communication (ECOC).
18. C. B. Gaur, V. Gordienko, F. Ferreira, V. Ribeiro, and N. J. Doran, "Fibre optic parametric amplifier for high-capacity burst-mode access networks," Opt. Express **29**(14), 21190–21198 (2021).
19. D. Uzunidis, M. Presi, A. Sgambelluri, F. Paolucci, A. Stavdas, and F. Cugini, "Bidirectional single-fiber filterless optical networks: modeling and experimental assessment," J. Opt. Commun. Netw. **13**(6), C1–C9 (2021).
20. M. E. Marhic, *Fibre optical parametric amplifiers, oscillators and related devices* (Cambridge University Press, 2008), Chap. 1.
21. L. K. P. Gordon and M. E. Marhic, "Amplification of DWDM channels at 1.28 Tb/s in a bidirectional fibre optical parametric amplifier," Opt. Express **22**(7), 8726–8733 (2014).
22. M. Jazayerifar, I. Sackey, R. Elschner, T. Richter, L. Molle, P. W. Berenguer, C. Schubert, K. Jamshidi, and K. Petermann, "Impact of Brillouin Backscattering on Signal Distortions in Single-Fibre Diversity Loop Based Polarization-Insensitive FOPAs," J. Lightwave Technol. **35**(19), 4137–4144 (2017).
23. C. B. Gaur, V. Gordienko, F. Bessin, and N. J. Doran, "Dual-Band Amplification of downstream L-band and upstream C-band signals by FOPA in extended reach PON," in 2020 European Conference on Optical Communications (ECOC).
24. V. Gordienko, C. B. Gaur, F. Bessin, I. D. Phillips, and N. J. Doran, "Robust polarization-insensitive C & L band FOPA with >17 dB gain for both WDM and bursty traffic," in 2021 Optical Fiber Communications Conference and Exhibition (OFC), paper M5B.3.
25. C. Gaur, V. Gordienko, and N. J. Doran, "Bi-directional C&L dual-band fiber optic parametric amplifier for reach extended access link," Aston University (2021), https://doi.org/10.17036/researchdata.aston.ac.uk.00000513.